Low cloud response to aerosol-radiation-cloud interactions: Idealized WRF numerical experiments for EUREC[4]A project

Nazario Tartaglione[1,2] | Fabien Desbiolles[1,3] | Anna del Moral-Méndez[1,4] |
Agostino N. Meroni[3] | Anna Napoli[1,5,6] | Matteo Borgnino[3] |
Antonio Parodi[1] | Claudia Pasquero[3,7]

[1]CIMA Research Foundation, Savona, Italy

[2]CSA, CN-CRE, ISPRA, Rome, Italy

[3]Department of Earth and Environmental Sciences, University of Milano-Bicocca, Milan, Italy

[4]National Center for Atmospheric Research, Boulder, Colorado, USA

[5]Department of Civil, Environmental and Mechanical Engineering, Università degli studi di Trento, Trento, Italy

[6]Center Agriculture Food Environment (C3A), Trento, Italy

[7]ISAC-CNR, Turin, Italy

Correspondence
Nazario Tartaglione, Italian Institute for Environmental Protection and Research, Rome 00144, Italy.
Email: nazario.tartaglione@isprambiente.it

Abstract

Aerosols significantly affect cloud microphysics and energy budget in different ways. The contribution of the direct, semi-direct, and indirect effects of aerosols on radiation are here investigated over the North Atlantic tropical ocean under different aerosol loadings. The Weather Research and Forecasting Model is used to perform a set of numerical idealized experiments, which are forced with prescribed aerosol profiles. We evaluate the effects of aerosols on modeled shallow clouds and surface radiative budget. The results indicate that large aerosol loadings are associated with enhanced cloudiness and reduced precipitation. While the change in rainfall is mainly due to the larger number of smaller droplets, the change in cloudiness is attributed to the effects of absorbing aerosols, mainly dust particles, which are responsible for a rise of temperature that feeds back onto specific humidity. As in the boundary layer the increase of moisture dominates, the net effect is a higher relative humidity, which favors the formation of thin low non-precipitating clouds. The feedback accounts for a dynamical change in the lower troposphere: shortwave radiation absorption increases temperature at the top of the marine atmospheric boundary-layer and reduces entrainment of warm and dry air, increasing low level moisture content. Despite the overall increase in cloudiness, daytime cloud cover is reduced. The semi-direct effect of aerosols on clouds results in a warming of the surface, opposite to the indirect effect.

KEYWORDS
aerosol-cloud interactions, aerosols, radiation-aerosol-cloud interactions, shallow clouds, Tropical Atlantic

---

Anna del Moral-Méndez, Anna Napoli, and Nazario Tartaglione are respectively at NCAR, University of Trento, and ISPRA now.

1 | INTRODUCTION

Shallow cumulus clouds, with their extensive cover of the low-latitude oceans, cool the planet by reflecting solar radiation (Bony et al., 2017). Radiative transfer in marine atmospheric boundary layer (MABL) clouds depends on their fine scale characteristics (Comstock et al., 2004; VanZanten & Stevens, 2005). Numerical models predict different low-level cloud responses to global warming, resulting in large uncertainties in climate sensitivity (Moreno-Chamarro et al., 2022; Yao & Del Genio, 2002; Zelinka et al., 2020). Among the many properties that affect cloud formation and evolution, aerosols play an important role. In presence of a high concentration of water-friendly particles acting as cloud condensation nuclei (CCN), a large number of small droplets are activated, leading to low auto conversion and collision rates, prolonging cloud lifetime (Albrecht, 1989), favoring evaporation when dry air is entrained in the cloud (Ackerman et al., 2004; Jiang et al., 2006), and modifying the release of latent heat, which drives the air buoyancy (Douglas & L'Ecuyer, 2021). While aerosols can also delay the onset precipitation (Lonitz et al., 2015; Spill et al., 2019), the change in rain mass with aerosol depends on environmental conditions, which affect droplet growth rate by collision and the evaporation rate (Douglas & L'Ecuyer, 2021; Khain et al., 2008; Lonitz et al., 2015).

Complex responses of low cloud cover to increased aerosols have also been reported (Ackerman et al., 2004; Chen et al., 2014; Christensen et al., 2020; Mardi et al., 2019; Stevens et al., 1998), as competing effects exist. For instance, a non-monotonic relationship between cloud fraction and aerosol loading emerges, with a positive correlation when the precipitation inhibition dominates, and a negative one at very large concentrations, as non-precipitating clouds evaporate more if droplets are smaller (Chen et al., 2014; Small et al., 2009; Xue et al., 2008). Also, overall liquid water response to increased CCN is set by the sum of the lower troposphere moistening effect directly related to the suppression of surface precipitation and of the drying effect from increased entrainment of overlying air, resulting in changes in the liquid water path of different sign depending on which process dominates (Ackerman et al., 2004; Sandu et al., 2008; Stevens et al., 1998). Aerosol-induced modification of condensation and evaporation can lead to latent heat warming and cooling at different levels in the air column, affecting the static stability of the cloud layer and thus the depth of convection (Dagan et al., 2017; Stevens & Feingold, 2009). This can result in a dipolar change of cloudiness at high and low levels in subtropical regions (Spill et al., 2019).

Most of the cited works focused on the aerosol indirect effects (IE) on radiation, that is, on the aerosol interactions with cloud microphysics, through the first IE (change in droplet concentration and size, that impacts instantaneous albedo; Twomey, 1974) and the second IE (change in cloud evolution, that impacts time averaged albedo; Albrecht, 1989; Penner et al., 2001). Aerosols impact cloud properties, and the radiative budget, also through the local warming induced by absorption of solar radiation, that change atmospheric stability (semi-direct effect, SDE) (Ackerman et al., 2000; Hansen et al., 1997; Koch & Del Genio, 2010). SDE is a major source of debate and uncertainty in the scientific community (Allen et al., 2019; Glotfelty et al., 2019; Pavlidis et al., 2020). For example, the global semi-direct radiative change corresponding to increased levels of absorbing aerosols leads to either cooling or warming of the climate system depending on the vertical aerosol atmospheric heating profile adopted in the model (Allen et al., 2019; Stjern et al., 2017).

Improvements rely upon the expansion of observational and modeling studies. While many studies to date have focused on continental regions, marine clouds are known to be of fundamental importance as they typically cover low albedo surfaces and their properties strongly influence the radiative budget. Due to the high cost of deploying appropriate platforms in the remote ocean, measurements of aerosols and clouds in the marine environment are sparser than over continents. The study of the relationship between aerosols and clouds in a region of strong insolation was one of the goals of the joint European-American EUREC[4]A[1]-ATOMIC effort (Quinn et al., 2021; Stevens et al., 2021). The field campaign took place in the Northwestern Tropical Atlantic (Figure 1a) between January and February 2020 and was characterized by the deployment of an unprecedented range of observing platforms, mainly to study the shallow convection associated with trade cumuli, which are prominent in winter in the area where the field campaign took place (Nuijens et al., 2015).

Although typical winter meteorological conditions do not include dust from North Africa, periods of long-range transport of African smoke and dust to Barbados, leading to a large increase in aerosol concentrations, were observed during the EUREC[4]A field campaign (Chazette et al., 2022; Gutleben et al., 2022; Royer et al., 2023). These observations motivated the choice of numerical simulations with very different aerosol forcings. We present results from high-resolution simulations in the EUREC[4]A region in winter, running with different process-activated options and different aerosol types and concentrations to study the interactions between aerosols, radiation and clouds. In Section 2, we describe the

setup of the simulations and we discuss the output of the control run focusing on the diurnal cycle in the low troposphere, then we present the sensitivity of the results to different aerosol loadings (Section 3), and finally we summarize the results (Section 4).

2 | STUDY APPROACH AND THE CHARACTERISTICS OF THE LOW TROPOSPHERE DAILY CYCLE

To investigate the effects of aerosols on low atmospheric dynamics in the subtropics, we focus on the characteristics of the mean daily cycle computed over a relatively extended period of time, that is, 1 month. Despite periods of large aerosol loading typically last for a few days, triggered by long-range transport from African fires and deserts, here we don't explicitly mimic such transport but instead we compare a control simulation with a low aerosol loading with idealized simulations that include aerosols with different characteristics. This allows us to consider the overall effects of aerosols under different environmental conditions, as it is known that considerable day to day meteorological variability exists (Savazzi et al., 2022, e.g., Figure S1). To this aim, we perform numerical simulations with the Advanced Research Weather Research and Forecasting (WRF) model V4.1.5 (Skamarock et al., 2019), in which the aerosol characteristics are prescribed. WRF solves the fully compressible non-hydrostatic Euler equations on an Arakawa C-grid with hybrid vertical coordinates. A complete description of the numerical configuration can be found in the supplementary materials. Briefly, a two-way nested

domain configuration is used (see Figure 1a), with a horizontal grid spacing of 9 km (D01) and 3 km (D02). The child domain encompasses the region sampled by the EUREC[4]A campaign (Stevens et al., 2021). The model is set up with 75 vertical levels, with 25 of them approximately below 2 km for a better representation of the MABL. Simulations are run for 3 months (December 2019 to February 2020), where the first 2 months are used as dynamical and aerosol loading spin up respectively and the full month of February is analyzed.

Initial and boundary conditions are prescribed from ERA5 hourly reanalysis (Hersbach et al., 2020) for atmospheric variables and from daily Multiscale Ultrahigh Resolution L4 analysis (Chin et al., 2017) for sea surface temperature (SST). The use of a daily SST field is justified by the fact that, in the trade wind regions, strong wind mixing in the upper ocean induces very slight diurnal SST variations (Brill & Albrecht, 1982; Vial et al., 2019). The large scale boundary conditions provided at the edges of the (relatively small) computational domain constrain the simulated fields to be consistent to ERA5 reanalysis throughout the whole duration of the simulation (see Figure S2). The microphysics scheme is Thompson Aerosol-Aware (Thompson & Eidhammer, 2014), which considers "water-friendly" (QNWFA, representing a combination of sulfates, sea salts, and organic matter) and "ice-friendly" particles (QNIFA, representing mineral dust). Idealized profiles of QNWFA and QNIFA are applied at the lateral boundaries of the coarse domain during January and February, to mimic the aerosol advection from large scale winds. In the control simulation, these boundary profiles correspond to a two-month (January–February) and D01 spatial average of the
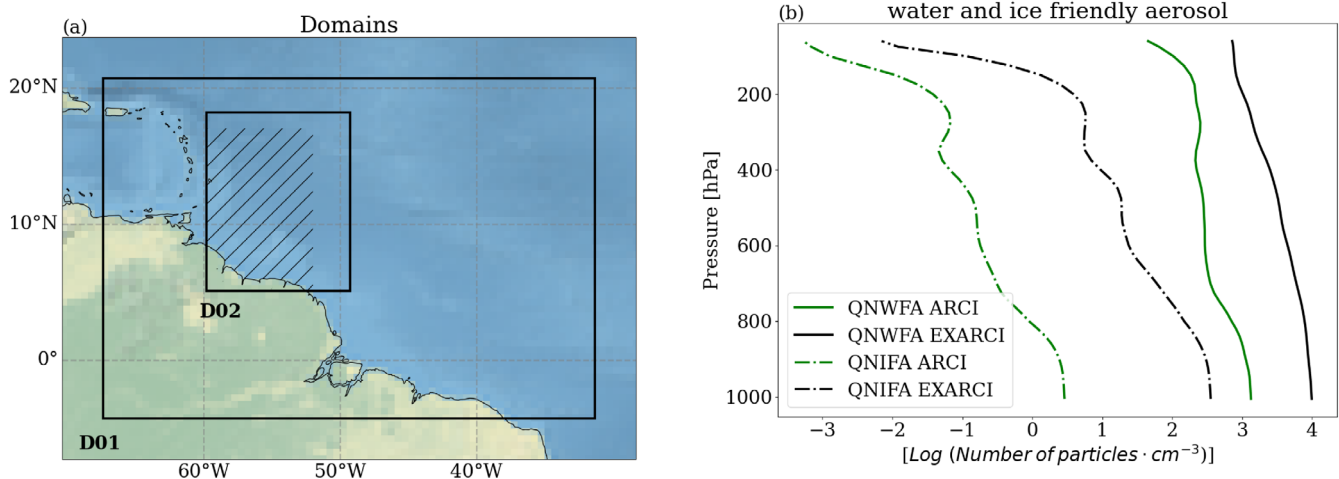

FIGURE 1 (a) WRF domains D01 and D02. The hatched area represents the region over which the analyses are performed. (b) Water (solid lines) and ice (dashed lines) friendly aerosol particle number concentration averaged on February in the analysis area, for ARCI and EXARCI experiments.

climatological profiles from Colarco et al. (2010). Aerosols enter into the RRTM radiation scheme (Iacono et al., 2008) in the experiment denoted as ARCI (aerosol-radiation-cloud interaction), while they only impact cloud microphysics in ACI (aerosol-cloud interaction) experiment. Owing to the low amount of aerosols in those simulations, the differences in the results between ARCI and ACI are minimal and are not discussed through the paper. For both configurations, high aerosol concentration simulations (named EXARCI and EXACI) are performed, where the lateral boundary profiles are obtained by multiplying the climatological ones by a factor of 100. This is a simplistic representation, which does not account for any change in the vertical level of peak concentration between background periods and long-range transport periods (Chazette et al., 2022). It is chosen as it allows us to compare the mean effect of the different aerosol loading over a range of wintertime meteorological conditions, while the inclusion of a time varying aerosol loading would mix the effects of aerosols with the effects of the day to day meteorological variability, hampering solid conclusions to be drawn. To partially account for changes in the fraction of particle types observed between background periods (dominated by marine aerosols) and long range transport events (dominated by African dust and smoke, Royer et al., 2023), we also run two simulations in which different types of aerosols are individually modified. In EXIFA experiment, only dust particles are increased to the high levels of EXARCI, and in EXWFA experiment, only aerosols acting as cloud condensation nuclei (mainly sulfates, sea salt, and organic matter) are increased to the high levels of EXARCI.

The resulting vertical profiles of February mean aerosol particle number concentration in the inner domain indicate that the lower troposphere contains about 10 times more particles in EXARCI, EXACI, and EXWFA than in ARCI, and ACI simulations (Figure 1b; Figure S3). In EXARCI, EXACI, and EXIFA runs, the number of dust particles is about two orders of magnitude larger than in ARCI and ACI experiments, reaching values that are about 30% of the total number of aerosols in the background experiments. It should be noticed that in EXIFA simulation the total number of aerosols (which is dominated by water friendly aerosols) is only slightly larger than in background conditions (ARCI and ACI). Despite the highly idealized representation of aerosol transport we use, the 10-fold increase of total aerosol concentration between the high aerosol loading case and the background conditions, as well as the fraction of dust particles in EXIFA experiments, are consistent with observational measurements in the region (Chazette et al., 2022; Royer et al., 2023).

Differences between EXARCI and ARCI simulation outputs are used to quantify the overall effects of the different aerosol loading. Comparison between EXACI and ACI allows us to isolate the effect of the change in the number of cloud condensation nuclei alone. Subtraction of this effect from the overall response provides an estimate of the direct and semi-direct effects of aerosols. Exploration of EXIFA and EXWFA outputs allow us to identify the role of different particle types.

Before focusing on those effects, we here describe the output of the control run (ARCI), and compare it with observational data. The diurnal cycle of cloud fraction (Figure 2a) is characterized by a maximum at night (04:00 local time, LT) and a minimum in the early afternoon (13:00 LT), in agreement with previous studies (Vial et al., 2019, 2023). This diurnal cycle is driven by near surface winds, which, in the model as well in the radio sound data collected during EUREC4A campaign (Stephan et al., 2021), peak at night (see Figure S4). The winds affect air-sea fluxes and thus impact on boundary layer characteristics. While near surface specific humidity increases in the afternoon, the lifting condensation level lowers and clouds form (cfr. Figure 4a; Figures S2a and S5). The increase in cloudiness at the top of the MABL favors long wave radiation trapping, decreasing the static stability and thus enhancing shallow convection mass flux (see Brunt-Väisälä frequency and maximum updraft velocity daily cycles in Figure 3c,d), with the result of thickening the cloud layer in the subsequent hours. Consistent with this interpretation, the simulated cloud top height and precipitation (mostly carried by stratocumulus clouds) peak at dawn, about 3 h after the peak in cloudiness near cloud base (Figures 2a and 3). The described characteristics of the low troposphere daily cycle are in agreement with observations collected during the EUREC4A campaign (Figure S4) and with the outcome of previous observational and modeling studies (Savazzi et al., 2022; Vial et al., 2019; Vial et al., 2023; Vogel et al., 2020), indicating that our simulations capture most of the relevant dynamics in the region.

3 | AEROSOL IMPACTS ON LOW TROPOSPHERE

The addition of aerosols suppresses precipitation at the surface: daily mean drizzle is reduced by more than two thirds in the simulations with a 10-fold increase of particles (EXARCI, EXACI, and EXWFA experiments) with respect to the control run (Figure 3a). This result is in line with the classical mechanism of rainfall reduction in warm clouds associated with the smaller (and more
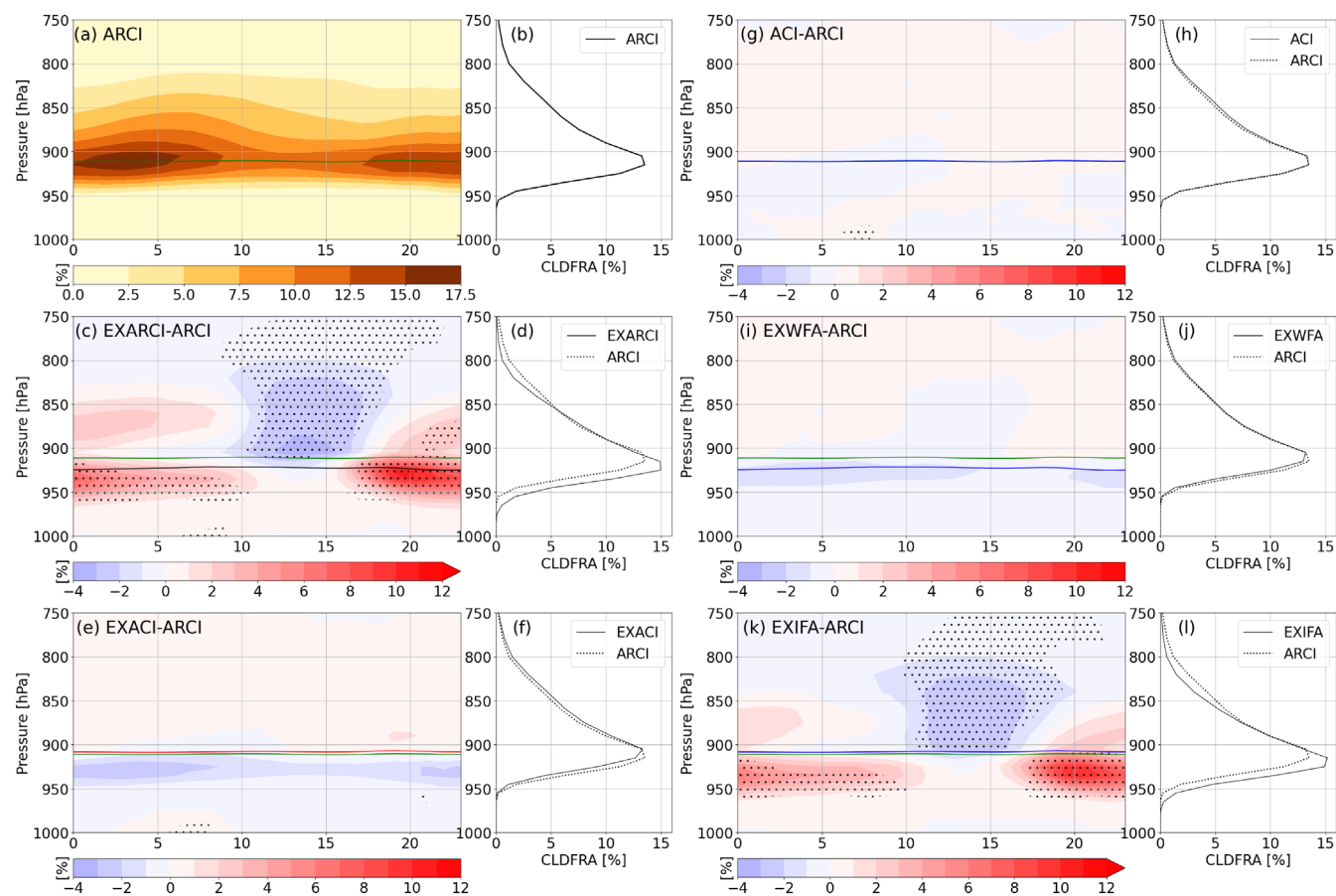
FIGURE 2 (Left panels) Daily cycle (in local time, UTC-4 h) of cloud fraction for (a) ARCI, and the associated anomalies of (c) EXARCI, (e) EXACI, (g) ACI, (i) EXWFA, and (k) EXIFA. Dotted area indicates statistically significant differences at the 5% confidence level, evaluated using the *t*-test. The solid lines in the figures denote the boundary layer height for ARCI (green), EXARCI (black), EXACI (red), and ACI (blue). (Right panels) Profiles of daily mean cloud fraction for (b) ARCI, (d) EXARCI, (f) EXACI, (h) ACI, (j) EXWFA, and (l) EXIFA.

numerous) droplets in polluted conditions, due to the larger number of cloud condensation nuclei (Sandu et al., 2008). The role played by CCN is further demonstrated by the results of the EXIFA experiment, in which the number of water friendly aerosols is the same as in ARCI: in this case the reduction of precipitation is limited to about one third. This experiment however also indicates that precipitation is, to a lesser degree, affected by processes other than the number of droplets. To shed light onto those, we now focus on other metrics computed in the different simulations.

Precipitation reduction is accompanied by different changes in cloud properties. Overall, the addition of aerosols in EXARCI and EXIFA significantly increases the daily mean cloud fraction, especially near cloud base (Figure 2c,d,k,l), but it has minor impacts in EXACI and in EXWFA (Figure 2e,f,i,j; Figure S6). This difference indicates that the larger number of cloud condensation nuclei is insufficient to explain the change in cloudiness obtained in EXARCI and EXIFA.

Peak daily mean cloud fraction (as well as MABL top pressure, Figure 3b) is located at 911 hPa in ARCI and ACI, at 921–925 hPa in EXARCI and EXIFA, and at 908 hPa in EXACI and EXWFA. A thicker MABL in an environment with many CCN has been found in previous studies, which attributed it to the enhanced entrainment of warm dry air at the top of the MABL (that leads to changes in water vapor and temperature), associated with the suppression of precipitation (Sandu et al., 2008; Stevens et al., 1998). This is in line with the results of EXACI and EXWFA, for which the MABL top height is slightly increased with respect to ACI and ARCI. Instead, the shallower MABL in EXARCI and EXIFA indicates that the interaction of radiation with aerosols (especially dust particles) triggers different processes.

The cloudiness change is not uniform throughout the day (Figure 2c). Cloud fraction near cloud base is significantly enhanced in EXARCI from midafternoon to the morning: during those hours it varies between 12% and

16% in the control (ARCI) and increases up to 22% in EXARCI. Cloud fraction above the boundary layer and below the inversion layer (i.e., cloudiness associated with shallow convection processes) shows instead a significant decrease in EXARCI during the central hours of the day. This results in an increased amplitude of shallow cloud fraction daily cycle. A correlated change in liquid water content is observed (Figure S7). The daily mean water vapor mixing ratio is also increased, with large moistening of the boundary layer throughout the day and of the layer above the MABL top especially during night-time (Figure 4b). The temperature in the lower atmosphere increases (Figure 4e), but not enough to maintain a constant relative humidity in the MABL, which increases by 4% from an average of 70% at the surface (Figure S8).
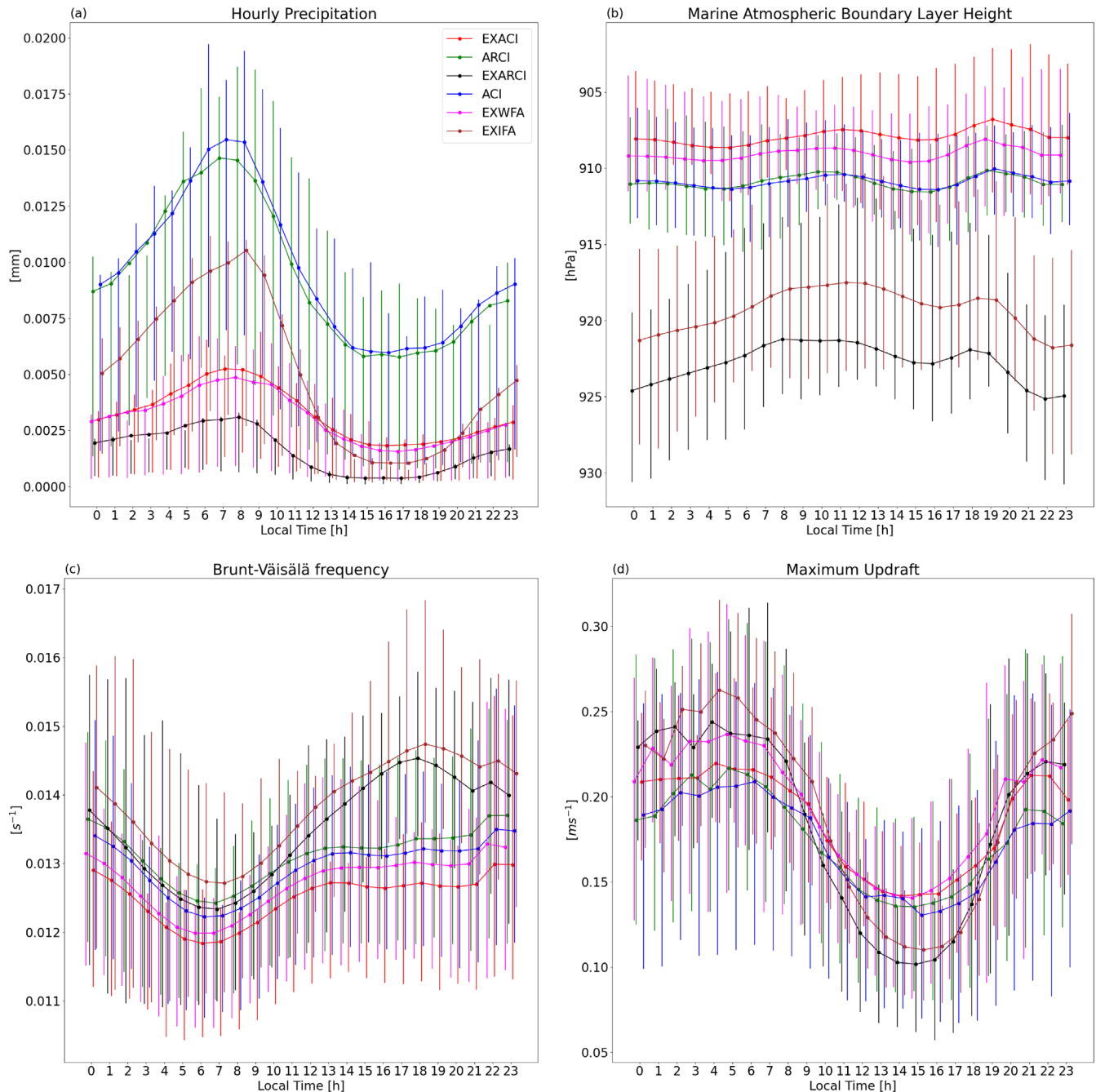

FIGURE 3 Daily cycle (in local time, UTC-4 h) of hourly precipitation (a), marine atmospheric boundary layer top pressure (b), Brunt-Väisälä frequency at 905 hPa (c), and maximum updraft velocity between 1000 and 750 hPa (d) for ARCI (green), EXARCI (black), ACI (blue), EXACI (red), EXWFA (magenta), and EXIFA (brown). The circles indicate the mean value and the bars indicate the interquartile range. It is represented in local time (UTC-4 h).
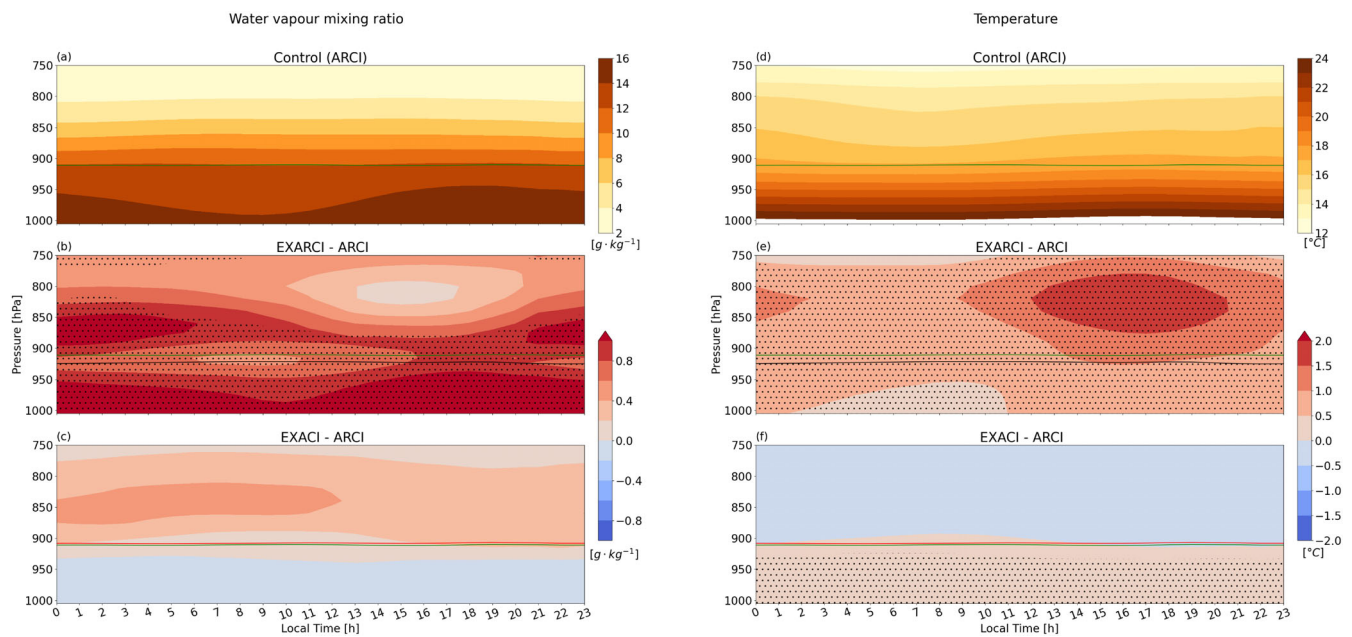
FIGURE 4 Daily cycle (in local time (UTC-4 h) of water vapor mixing ratio for ARCI (a) and its anomalies with EXARCI and EXACI (b, c) together with the daily cycle of temperature in ARCI (d), and its anomalies with EXARCI and EXACI (e, f). Dotted area indicates statistically significant differences at the 5% confidence level, evaluated using the *t*-test. The solid lines in the figures denote the boundary layer height for ARCI (green), EXARCI (black), and EXACI (red).

The large warming in EXARCI with respect to ARCI located in the afternoon between 900 hPa and 800 hPa (Figure 4e) suggests that shortwave radiation absorption in those layers is responsible for the modeled temperature increase. This interpretation is confirmed by the much smaller positive temperature anomaly in EXACI, mainly confined to the MABL (Figure 4f) and related to reduced evaporation of drizzle and to enhanced entrainment of warm air from above (Sandu et al., 2008; Stevens et al., 1998). In EXARCI, the warming above the MABL favors droplet evaporation, cloud fraction reduction, and further suppression of drizzle (Figures 2b and 3a). We also note that the warming is smaller in the MABL than above it, probably due to the large extinction of shortwave radiation by the aerosol particles above. The differential warming at different heights modifies the temperature lapse rate, stabilizing the air column in the afternoon (see the Brünt-Väisäla frequency in Figure 3c) and thus inhibiting exchanges between the boundary layer and the drier air aloft. In fact, maximum updraft velocity is reduced by about 30% at 15:00 local time (Figure 3d), and the MABL is shallower in EXARCI (Figure 3b). This process in EXARCI counteracts and dominates over the effect of increased CCN on entrainment rate associated with the reduced liquid water flux, which is dominant in the EXACI and EXWFA response. Consequently, MABL water vapor mixing ratio and relative humidity increase (Figure 4b; Figure S8), favoring

droplet formation at lower levels (the lifting condensation level decreases, Figure S6) and promoting more (non-precipitating) stratus clouds. At the same time, enhanced absorption of longwave radiation slightly warms the lower levels (Figure 4e). During nighttime, owing to the absence of shortwave radiation, entrainment rate changes are driven by the suppression of precipitation: updrafts and stratocumulus clouds increase (Figures 3d and 4b). These processes result in a negative correlation between MABL thickness and water vapor mixing ratio (Figure S9): less entrainment of dry air at the top of the boundary layer increases water vapor content in the MABL and decreases MABL height. As a result, in EXARCI the daily cycle of shallow convection and of cloudiness is amplified.

The aerosol modulation of lower atmosphere static stability (through shortwave radiation absorption during daytime) and the suppression of precipitation (mainly associated to the large number of cloud droplets but also amplified by the evaporation of stratocumulus clouds during daytime) represent the main drivers of the differences of low cloud evolution between EXARCI and ARCI simulations. The similarity of the cloud daily cycle between EXARCI and EXIFA experiments, and the difference with respect to EXWFA experiment (Figure 3; Figure S6) indicate that dust particles, through their peculiar optical properties, are the aerosol type that triggers the described response.
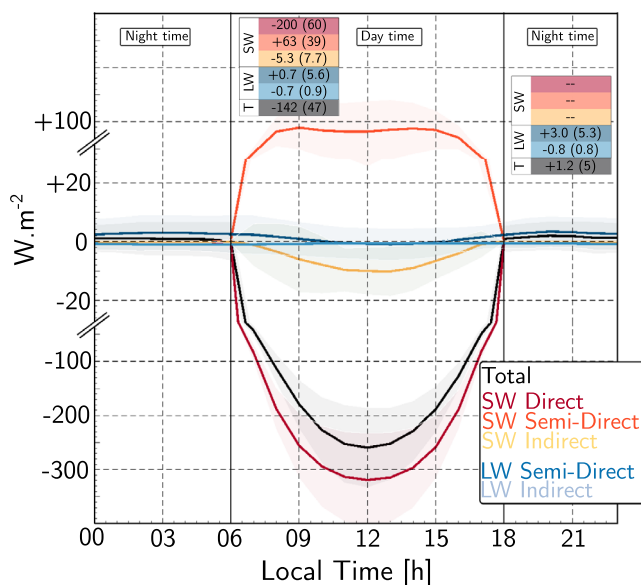
FIGURE 5 Daily cycle of surface radiative budget changes (black dotted line) and relative contributions of the direct, semi-direct, and indirect effects on short waves in red, orange, and yellow, respectively; relative contribution of semi-direct and indirect effect on longwave radiation in blue and light blue, respectively. For clarity of the figure, the y-axis has been set with two different scaling for the low and high ranges, respectively. The tables incorporated in the figure indicate the mean and the hourly standard deviation of each effect in the surface radiative budget ($W.m^{-2}$) for day and night time, respectively. Indirect effects are estimated as the difference between EXACI and ACI radiative budgets. Direct effects are estimated as the difference between EXARCI and ARCI budgets in clear sky conditions. Semidirect effects are estimated as the difference between EXARCI and ARCI budget difference between all sky and clear sky conditions, upon further removal of the indirect effects.

In closing this section, we quantify the radiative effects of the low-cloud cover change associated with the excess aerosol loading (Figure 5). Details on their computation are provided in supplementary materials. Indirect effects (computed by comparing the differences between EXACI and ACI) account for a small reduction (not statistically significant at the 95% confidence level) in downward shortwave radiation at the surface (Sandu et al., 2008). When aerosol-radiation interactions are activated, increased aerosol concentration greatly reduces downward shortwave radiation at the surface. The direct effect of the excess aerosols (computed by comparing the clear sky surface radiation difference between EXARCI and ARCI) is associated with instantaneous anomalies up to $-300\ W \cdot m^{-2}$ (and a daily mean reduction of $100\ W \cdot m^{-2}$). This corresponds to a relative increase of shortwave radiation extinction by aerosols of about 38%, a value that can be considered to correspond to high aerosol loadings, common in polluted areas (Liu et al., 2007) and somehow higher than what

reported in recent studies in the EUREC⁴A region during the two observed aerosol outbrake periods, when the aerosol extinction of radiation was increased by about 25% with respect to the background periods (Chazette et al., 2022). The semidirect effect of the excess aerosol loading (computed from the EXARCI-ARCI differences between all sky and clear sky budgets, which allow the quantification of radiation extinction associated to the change in cloudiness) accounts for an increase of solar radiation reaching the surface up to $75\pm40\ W \cdot m^{-2}$, with a daily mean of $34\pm18\ W \cdot m^{-2}$. Small changes are also observed in surface net longwave radiation, with minimal variations during daytime and a warming effect at night (Figure 5).

Overall, aerosols cause a reduction of sunlight at the surface (through their large direct effect), but the semidirect effect strongly mitigates the extinction of shortwave radiation. Despite the fact that the precise numbers given above depend on the optical properties of aerosols represented in the simulation, we conclude that SDEs can have an impact on the radiation budget much larger than the IEs, and of opposite sign. In other words, despite the overall daily mean increase in cloudiness in EXARCI (and in EXIFA), the daytime reduction of clouds above the MABL due to the evaporation of droplets in presence of sunlight absorption by dust particles increases the light propagated to the surface with respect to the case in which SDE is not accounted for.

4 | CONCLUDING REMARKS

In this paper we presented cloud resolving numerical experiments performed with the WRF model forced at the boundaries by idealized aerosol profiles and meteorological conditions of the EUREC⁴A field campaign in the Northwest Tropical Atlantic between January and February 2020. We analyzed the response of the lower troposphere to increased aerosol concentration (by a factor of 10 with respect to the climatology), and to changes in the concentration of specific particle types (water friendly aerosols and dust particles, separately). Direct, indirect, and semi-direct effects on radiation were separately analyzed, with the use of different numerical simulations accounting and not accounting for aerosol-radiation interactions with shallow clouds.

The large sensitivity of cloud fraction to aerosol concentration and type found in this work extends the results obtained by Gupta et al. (2022), where it was shown that aerosol characteristics can be more important than meteorological variables in driving cloud properties.

The results indicate that with the excess aerosol loading (whose radiative effects correspond to those of a

heavy pollution event), daily mean cloud cover is increased and precipitation is suppressed. While the effects on precipitation can be ascribed to the classical increase in warm cloud lifetime due to the presence of many small (non-precipitating) droplets and is largely related to the action of aerosols as cloud condensation nuclei, the changes in cloud fraction are mainly a consequence of aerosol absorption and scattering of shortwave radiation by dust particles. Consistent with Gryspeerdt et al. (2016), we find that the relationship between aerosol loading and cloud fraction is not dominated by the change in the number of droplets but rather by the increased specific humidity in the boundary layer.

In presence of large concentrations of dust particles, a strong warming of the layer above the MABL during daytime is responsible for the evaporation of stratocumulus clouds and for the increased static stability above the boundary layer. This reduces the mass exchanges between the MABL and the warm and dry air aloft. Increased moisture in the shallower MABL favors the formation of thin clouds, resulting in a dipolar change of cloudiness at different vertical levels. The aerosol ability to function as CCN partially counteracts this effect, as the associated suppression of precipitation enhances entrainment of warm and dry air. Given that this is a minor effect in presence of shortwave radiation and is significant only at night, it results in a marginal daily mean effect and MABL humidity is enhanced throughout the day.

Despite the overall increase of cloudiness, the reduction of liquid water path during daylight associated with the evaporation of stratocumulous clouds significantly lessens the extinction of shortwave radiation due to aerosol scattering and absorption (by about 30%). While aerosol IE only generate a minor albedo increase (Sandu et al., 2008), the SDE of dust particles can lead to a significant reduction of albedo.

The results presented in this work are worth to be linked to the study of Perlwitz and Miller (2010), who used a general circulation atmospheric model and reported a counter-intuitive feedback linking the atmospheric heating induced by tropospheric absorbing aerosol to an increase in cloud cover (especially low-level clouds). They highlighted that higher levels of aerosol absorption are responsible for two counteracting processes: a greater diabatic heating that warms the atmospheric column (decreasing relative humidity) and an increase in water vapor mixing ratio that can outweigh the temperature effect on relative humidity. The net result of the increased aerosol absorption is an increment in relative humidity and an increase in low cloud cover. The higher specific humidity in their work is linked to an enhanced moisture convergence associated with the large scale dynamical response to radiative heating. In our work, a similar (but local) feedback is at play, where the diabatic heating generates warming and cloud evaporation during daytime and at the same time modifies the dynamics by increasing the stability of the low troposphere, reducing the entrainment of dry air from above and resulting in an increase of specific humidity in the MABL, which increases low cloud fraction, especially at night.

In closing, we highlight important limitations of the study. The relevance of the presented aerosol-radiation feedback might be linked to the specific area and time interval analyzed. Sensitivity to large scale conditions has not been investigated and during the analyzed period no heavy precipitation event occurred, during which different processes than the ones related to drizzle here described might dominate. A thorough investigation of the sensitivity of the results to different aerosol optical properties has not been done. In particular, only changes to the concentrations of dust particles and of a mixture of water friendly aerosols (mainly sulfates and organic matter particles) have been implemented. The explicit representation of black and brown carbon would provide a useful extension of this work, especially given that biomass burning aerosols have been observed to be associated to the long range transport of African dust in the region. Also, our model uses prescribed SST, which does not account for the effects of shortwave radiation changes on the surface. Considering that the described processes depend on entrainment rate, it would be useful to run LES simulations that better represent it. Further work would be necessary to identify the relevant processes that account for variability in subtropical low cloud cover, that is ultimately associated to large changes in the energy budget of the Earth (Latham et al., 2008).

AUTHOR CONTRIBUTIONS

Nazario Tartaglione: Data curation; investigation; methodology; software; validation; visualization; writing – original draft; writing – review and editing. **Fabien Desbiolles:** Conceptualization; formal analysis; investigation; methodology; visualization; writing – original draft; writing – review and editing. **Anna del Moral-Méndez:** Data curation; investigation; methodology; writing – review and editing. **Agostino Meroni:** Conceptualization; investigation; methodology; writing – review and editing. **Anna Napoli:** Investigation; writing – review and editing. **Matteo Borgnino:** Investigation; visualization; writing – review and editing. **Antonio Parodi:** Conceptualization; funding acquisition; investigation; methodology; project administration; resources; supervision; writing – original draft; writing – review and editing. **Claudia Pasquero:** Conceptualization; funding acquisition; investigation; methodology;

CONFLICT OF INTEREST STATEMENT

The authors declare there are no conflicts of interests.

DATA AVAILABILITY STATEMENT

Experiments can be replicated using the WRF model (https://www.mmm.ucar.edu/models/wrf) with hourly ERA5 data as initial and boundary conditions, which can be downloaded from ECMWF (https://www.ecmwf.int). Sea Surface Temperature used in this study can be downloaded from https://podaac.jpl.nasa.gov/dataset/MUR-JPL-L4-GLOB-v4.1. Aerosol profiles applied to boundary of D01 can be found here https://github.com/nazariotart/EUREC4A/tree/main. The WRF output data that support the findings of this study are available from the corresponding author upon reasonable request.

ORCID

Nazario Tartaglione 🔟 https://orcid.org/0000-0002-9863-4161

ENDNOTE

[1] ElUcidating the RolE of Cloud-Circulation Coupling in ClimAte and Atlantic Tradewind Ocean–atmosphere Mesoscale Interaction Campaign.

REFERENCES

Ackerman, A.S., Kirkpatrick, M.P., Stevens, D.E. & Toon, O.B. (2004) The impact of humidity above stratiform clouds on indirect aerosol climate forcing. *Nature*, 432, 1014–1017. Available from: https://doi.org/10.1038/nature03174

Ackerman, A.S., Toon, O.B., Stevens, D.E., Heymsfield, A.J., Ramanathan, V. & Welton, E.J. (2000) Reduction of tropical cloudiness by soot. *Science*, 288, 1042–1047. Available from: https://doi.org/10.1126/science.288.5468.1042

Albrecht, B.A. (1989) Aerosols, cloud microphysics, and fractional cloudiness. *Science*, 245, 1227–1230. Available from: https://doi.org/10.1126/science.245.4923.1227

Allen, R.J., Amiri-Farahani, A., Lamarque, J.-F., Smith, C., Shindell, D., Hassan, T. et al. (2019) Observationally constrained aerosol–cloud semi-direct effects. *NPJ Climate and Atmospheric Science*, 2, 16. Available from: https://doi.org/10.1038/s41612-019-0073-9

Bony, S., Stevens, B., Ament, F., Bigorre, S., Chazette, P., Crewell, S. et al. (2017) EUREC4A: a field campaign to elucidate the couplings between clouds, convection and circulation. *Surveys in Geophysics*, 38, 1529–1568. Available from: https://doi.org/10.1007/s10712-017-9428-0

Brill, K. & Albrecht, B. (1982) Diurnal variation of the trade-wind boundary layer. *Monthly Weather Review*, 110, 601–613. Available from: https://doi.org/10.1175/1520-0493(1982)110<0601:DVOTTW>2.0.CO;2

Chazette, P., Baron, A. & Flamant, C. (2022) Mesoscale spatio-temporal variability of airborne lidar-derived aerosol properties in the Barbados region during EUREC4A. *Atmospheric Chemistry and Physics*, 22, 1271–1292. Available from: https://doi.org/10.5194/acp-22-1271-2022

Chen, Y.-C., Christensen, M.W., Stephens, G.L. & Seinfeld, J.H. (2014) Satellite-based estimate of global aerosol–cloud radiative forcing by marine warm clouds. *Nature Geoscience*, 7, 643–646. Available from: https://doi.org/10.1038/ngeo2214

Chin, T.M., Vazquez-Cuervo, J. & Armstrong, E.M. (2017) A multi-scale high-resolution analysis of global sea surface temperature. *Remote Sensing of Environment*, 200, 154–169. Available from: https://doi.org/10.1016/j.rse.2017.07.029

Christensen, M.W., Jones, W.K. & Stier, P. (2020) Aerosols enhance cloud lifetime and brightness along the stratus-to-cumulus transition. *Proceedings of the National Academy of Sciences*, 117, 17591–17598. Available from: https://doi.org/10.1073/pnas.1921231117

Colarco, P., da Silva, A., Chin, M. & Diehl, T. (2010) Online simulations of global aerosol distributions in the nasa geos-4 model and comparisons to satellite and ground-based aerosol optical depth. *Journal of Geophysical Research: Atmospheres*, 115, D14207. Available from: https://doi.org/10.1029/2009JD012820

Comstock, K., Wood, R., Yuter, S. & Bretherton, C. (2004) Reflectivity and rain rate in and below drizzling stratocumulus. *Quarterly Journal of the Royal Meteorological Society*, 130, 2891–2918. Available from: https://doi.org/10.1256/qj.03.187

Dagan, G., Koren, I., Altaratz, O. & Heiblum, R.H. (2017) Time-dependent, non-monotonic response of warm convective cloud fields to changes in aerosol loading. *Atmospheric Chemistry and Physics*, 17, 7435–7444. Available from: https://acp.copernicus.org/articles/17/7435/2017/, https://doi.org/10.5194/acp-17-7435-2017

Douglas, A. & L'Ecuyer, T. (2021) Global evidence of aerosol-induced invigoration in marine cumulus clouds. *Atmospheric Chemistry and Physics*, 21, 15103–15114. Available from: https://doi.org/10.5194/acp-21-15103-2021

Glotfelty, T., Alapaty, K., He, J., Hawbecker, P., Song, X. & Zhang, G. (2019) The weather research and forecasting model with aerosol–cloud interactions (wrf-aci): development, evaluation, and initial application. *Monthly Weather Review*, 147, 1491–1511. Available from: https://doi.org/10.1175/MWR-D-18-0267.1

Gryspeerdt, E., Quaas, J. & Bellouin, N. (2016) Constraining the aerosol influence on cloud fraction. *Journal of Geophysical Research: Atmospheres*, 121, 3566–3583. Available from: https://doi.org/10.1002/2015JD023744

Gupta, S., McFarquhar, G.M., O'Brien, J.R., Poellot, M.R., Delene, D.J., Miller, R.M. et al. (2022) Factors affecting precipitation formation and precipitation susceptibility of marine stratocumulus with variable above- and below-cloud aerosol concentrations over the Southeast Atlantic. *Atmospheric Chemistry and Physics*, 22, 2769–2793. Available from: https://doi.org/10.5194/acp-22-2769-2022

Gutleben, M., Groß, S., Heske, C. & Wirth, M. (2022) Wintertime saharan dust transport towards the caribbean: an airborne lidar case study during EUREC4A. *Atmospheric Chemistry and Physics*, 22, 7319–7330. Available from: https://doi.org/10.5194/acp-22-7319-2022

Hansen, J.E., Sato, M. & Ruedy, R. (1997) Radiative forcing and climate response. *Journal of Geophysical Research*, 102, 6831–6864. Available from: https://doi.org/10.1029/96JD03436

Hersbach, H., Bell, B., Berrisford, P., Hirahara, S., Horányi, A., Muñoz-Sabater, J. et al. (2020) The ERA5 global reanalysis. *Quarterly Journal of the Royal Meteorological Society*, 146, 1999–2049. Available from: https://doi.org/10.1002/qj.3803

Iacono, M.J., Delamere, J.S., Mlawer, E.J., Shephard, M.W., Clough, S.A. & Collins, W.D. (2008) Radiative forcing by long-lived greenhouse gases: calculations with the aer radiative transfer models. *Journal of Geophysical Research: Atmospheres*, 113, D13103. Available from: https://doi.org/10.1029/2008JD009944

Jiang, H., Xue, H., Teller, A., Feingold, G. & Levin, Z. (2006) Aerosol effects on the lifetime of shallow cumulus. *Geophysical Research Letters*, 33, L14806. Available from: https://doi.org/10.1029/2006GL026024

Khain, A.P., BenMoshe, N. & Pokrovsky, A. (2008) Factors determining the impact of aerosols on surface precipitation from clouds: an attempt at classification. *Journal of the Atmospheric Sciences*, 65, 1721–1748. Available from: https://doi.org/10.1175/2007JAS2515.1

Koch, D. & Del Genio, A.D. (2010) Black carbon semi-direct effects on cloud cover: review and synthesis. *Atmospheric Chemistry and Physics*, 10, 7685–7696. Available from: https://doi.org/10.5194/acp-10-7685-2010

Latham, J., Rasch, P., Chen, C.-C., Kettles, L., Gadian, A., Gettelman, A. et al. (2008) Global temperature stabilization via controlled albedo enhancement of low-level maritime clouds. *Philosophical Transactions of the Royal Society A: Mathematical, Physical and Engineering Sciences*, 366, 3969–3987. Available from: https://doi.org/10.1098/rsta.2008.0137

Liu, J., Xia, X., Wang, P., Li, Z., Zheng, Y., Cribb, M. et al. (2007) Significant aerosol direct radiative effects during a pollution episode in northern China. *Geophysical Research Letters*, 34, L23808.

Lonitz, K., Stevens, B., Nuijens, L., Sant, V., Hirsch, L. & Seifert, A. (2015) The signature of aerosols and meteorology in long-term cloud radar observations of trade wind cumuli. *Journal of the Atmospheric Sciences*, 72, 4643–4659. Available from: https://doi.org/10.1175/JAS-D-14-0348.1

Mardi, A.H., Dadashazar, H., MacDonald, A.B., Crosbie, E., Coggon, M.M., Aghdam, M.A. et al. (2019) Effects of biomass burning on stratocumulus droplet characteristics, drizzle rate, and composition. *Journal of Geophysical Research: Atmospheres*, 124, 12301–12318. Available from: https://doi.org/10.1029/2019JD031159

Moreno-Chamarro, E., Caron, L.-P., Loosveldt Tomas, S., Vegas-Regidor, J., Gutjahr, O., Moine, M.-P. et al. (2022) Impact of increased resolution on long-standing biases in highresmip-primavera climate models. *Geoscientific Model Development*, 15, 269–289. Available from: https://doi.org/10.5194/gmd-15-269-2022

Nuijens, L., Medeiros, B., Sandu, I. & Ahlgrimm, M. (2015) The behavior of trade-wind cloudiness in observations and models: the major cloud components and their variability. *Journal of Advances in Modeling Earth Systems*, 7, 600–615. Available from: https://doi.org/10.1002/2014MS000390

Pavlidis, V., Katragkou, E., Prein, A., Georgoulias, A.K., Kartsios, S., Zanis, P. et al. (2020) Investigating the sensitivity to resolving aerosol interactions in downscaling regional model experiments with wrfv3.8.1 over europe. *Geoscientific Model Development*, 13, 2511–2532. Available from: https://doi.org/10.5194/gmd-13-2511-2020

Penner, J., Andreae, M., Annegarn, H., Barrie, L., Feichter, J., Hegg, D. et al. (2001) *Aerosols, their direct and indirect effects climate change 2001: the scientific basis. contribution of working group I to the third assessment report of the intergovernmental panel on climate change.* Cambridge, UK, and New York, NY: Cambridge University Press, pp. 289–348.

Perlwitz, J. & Miller, R.L. (2010) Cloud cover increase with increasing aerosol absorptivity: a counterexample to the conventional semidirect aerosol effect. *Journal of Geophysical Research: Atmospheres*, 115, D08203. Available from: https://doi.org/10.1029/2009JD012637

Quinn, P.K., Thompson, E.J., Coffman, D.J., Baidar, S., Bariteau, L., Bates, T.S. et al. (2021) Measurements from the RV Ronald H. Brown and related platforms as part of the Atlantic Trade-wind Ocean-atmosphere mesoscale interaction campaign (ATOMIC). *Earth System Science Data*, 13, 1759–1790. Available from: https://doi.org/10.5194/essd-13-1759-2021

Royer, H.M., Pöhlker, M.L., Krüger, O., Blades, E., Sealy, P., Lata, N.N. et al. (2023) African smoke particles act as cloud condensation nuclei in the wintertime tropical North Atlantic boundary layer over Barbados. *Atmospheric Chemistry and Physics*, 23, 981–998. Available from: https://doi.org/10.5194/acp-23-981-2023

Sandu, I., Brenguier, J., Geoffroy, O., Thouron, O. & Masson, V. (2008) Aerosol impacts on the diurnal cycle of marine stratocumulus. *Journal of the Atmospheric Sciences*, 65, 2705–2718. Available from: https://doi.org/10.1175/2008JAS2451.1

Savazzi, A.C.M., Nuijens, L., Sandu, I., George, G. & Bechtold, P. (2022) The representation of the trade winds in ecmwf forecasts and reanalyses during eurec[4]a. *Atmospheric Chemistry and*

Physics, 22, 13049–13066. Available from: https://doi.org/10.5194/acp-22-13049-2022

Skamarock, W.C., Klemp, J.B., Dudhia, J., Gill, D.O., Liu, Z., Berner, J. et al. (2019) *A description of the advanced research WRF version 4.* Boulder, CO: NCAR Tech. Note NCAR/TN-556+STR, p. 145. Available from: https://doi.org/10.5065/1dfh-6p97

Small, J.D., Chuang, P.Y., Feingold, G. & Jiang, H. (2009) Can aerosol decrease cloud lifetime? *Geophysical Research Letters*, 36, L16806. Available from: https://doi.org/10.1029/2009GL038888

Spill, G., Stier, P., Field, P.R. & Dagan, G. (2019) Effects of aerosol in simulations of realistic shallow cumulus cloud fields in a large domain. *Atmospheric Chemistry and Physics*, 19, 13507–13517. Available from: https://doi.org/10.5194/acp-19-13507-2019

Stephan, C.C., Schnitt, S., Schulz, H., Bellenger, H., De Szoeke, S.P., Acquistapace, C. et al. (2021) Ship-and Island-based atmospheric soundings from the 2020 eurec4a field campaign. *Earth System Science Data,* 13, 491–514. Available from: https://doi.org/10.5194/essd-13-491-2021

Stevens, B., Cotton, W.R., Feingold, G. & Moeng, C.-H. (1998) Large-eddy simulations of strongly precipitating, shallow, stratocumulus-topped boundary layers. *Journal of the Atmospheric Sciences*, 55, 3616–3638. Available from: https://doi.org/10.1175/1520-0469(1998)055<3616:LESOSP>2.0.CO;2

Stevens, B. & Feingold, G. (2009) Untangling aerosol effects on clouds and precipitation in a buffered system. *Nature*, 461, 607–613. Available from: https://doi.org/10.1038/nature08281

Stevens, B., Bony, S., Farrell, D., Ament, F., Blyth, A., Fairall, C. et al. (2021) Eurec⁴A. *Earth System Science Data*, 13, 4067–4119. Available from: https://doi.org/10.5194/essd-13-4067-2021

Stjern, C.W., Samset, B.H., Myhre, G., Forster, P.M., Hodnebrog, Ø., Andrews, T. et al. (2017) Rapid adjustments cause weak surface temperature response to increased black carbon concentrations. *Journal of Geophysical Research: Atmospheres*, 122, 11–462. Available from: https://doi.org/10.1002/2017JD027326

Thompson, G. & Eidhammer, T. (2014) A study of aerosol impacts on clouds and precipitation development in a large winter cyclone. *Journal of the Atmospheric Sciences*, 71, 3636–3658. Available from: https://doi.org/10.1175/JAS-D-13-0305.1

Twomey, S. (1974) Pollution and the planetary albedo. *Atmospheric Environment (1967)*, 8, 1251–1256. Available from: https://doi.org/10.1016/0004-6981(74)90004-3

VanZanten, M.C. & Stevens, B. (2005) Observations of the structure of heavily precipitating marine stratocumulus. *Journal of the Atmospheric Sciences*, 62, 4327–4342. Available from: https://doi.org/10.1175/JAS3611.1

Vial, J., Albright, A.L., Vogel, R., Musat, I. & Bony, S. (2023) Cloud transition across the daily cycle illuminates model responses of trade cumuli to warming. *Proceedings of the National Academy of Sciences of the United States of America*, 120, e2209805120. Available from: https://doi.org/10.1073/pnas.2209805120

Vial, J., Vogel, R., Bony, S., Stevens, B., Winker, D.M., Cai, X. et al. (2019) A new look at the daily cycle of trade wind cumuli. *Journal of Advances in Modeling Earth Systems*, 11, 3148–3166. Available from: https://doi.org/10.1029/2019MS001746

Vogel, R., Bony, S. & Stevens, B. (2020) Estimating the shallow convective mass flux from the subcloud-layer mass budget. *Journal of the Atmospheric Sciences*, 77, 1559–1574. Available from: https://doi.org/10.1175/JAS-D-19-0135.1

Xue, H., Feingold, G. & Stevens, B. (2008) Aerosol effects on clouds, precipitation, and the organization of shallow cumulus convection. *Journal of the Atmospheric Sciences*, 65, 392–406. Available from: https://doi.org/10.1175/2007JAS2428.1

Yao, M.-S. & Del Genio, A.D. (2002) Effects of cloud parameterization on the simulation of climate changes in the giss gcm. Part ii: sea surface temperature and cloud feedbacks. *Journal of Climate*, 15, 2491–2503. Available from: https://doi.org/10.1175/1520-0442(2002)015<2491:EOCPOT>2.0.CO;2

Zelinka, M.D., Myers, T.A., McCoy, D.T., Po-Chedley, S., Caldwell, P.M., Ceppi, P. et al. (2020) Causes of higher climate sensitivity in cmip6 models. *Geophysical Research Letters*, 47, e2019GL085782. Available from: https://doi.org/10.1029/2019GL085782

SUPPORTING INFORMATION

Additional supporting information can be found online in the Supporting Information section at the end of this article.